



UNIVERSITY OF
BIRMINGHAM

Medical Image Processing with Quadrees

School of Computer Science
University of Birmingham

Josh Wainwright

Supervisor: Iain Styles

Date: September 2014

Abstract

This study deduces that reionization began at a redshift of $z = 17.82(+3.06, -2.4)$ and ended at a redshift of $z = 7 \pm 1.8$. This is calculated by directly applying the dynamics of star formation and the ionization rate of neutral hydrogen in the Inter-galactic Medium. A photometry strategy consisting of 3 multi-band surveys is proposed in order to observe Lyman Break Galaxies across redshifts 6–17. The surveys will locate 100.5 ± 37.0 , 138.7 ± 100.6 , 358.1 ± 158.6 galaxies in redshift ranges 6–8.5, 8.5–10 and 10–17 respectively. These surveys will be completed by the James Webb Space Telescope and Euclid which are planned for launch in the coming decade. A follow up spectroscopy survey will be used to confirm the redshift and properties of 24, 4 and 48 galaxies in these 3 surveys respectively. The spectroscopy will be carried out using James Webb Space Telescope and a combination of single and multi-slit spectroscopy. It is shown that the use of known gravitational lenses, located between redshift 0.5–0.7, is very beneficial for discovering high redshift candidates as it can increase the depth of surveys by up to 3 magnitudes.

Table of Contents

Abstract	i
Table of Contents	ii
I Introduction	1
1 Medical Imaging	1
2 Sub-Diffraction-Limit Imaging	1
2.1 Image Manipulation	1
3 Benchmarking	1
II Data Structures	1
1 Simple Grid Method	2
2 Quadtrees	3
2.1 Morton Code	3
2.2 Hilbert Order	3
2.3 Gray Codes	4
2.4 Quadtree Definitions	4
3 Cluster Analysis	5
3.1 Rolling Ball Analysis	5
4 Quadtree Traversal	5
III ImageJ Plugin	5
1 ImageJ	6
2 ImageJ Plugin	6
Appendices	8
A Data File Structure	8

Part I

Introduction

1 Medical Imaging

In various scientific fields, viewing and imaging objects smaller than the human eye can naturally observe is an ability eagerly sought. Microscopy in medical fields has allowed us to learn about the nature of tissues, micro-organisms and cells and the way they work together and to develop preventative measures and cures for injuries and diseases.

The humble microscope, used as far back as the 1500's, is able to show us a world that is not usually visible, but in recent times, as our understanding has grown, we have desired to see beyond what ordinary microscopes are capable and have invented machines that let us catch a glimpse of some of the smallest structures, molecules. However, when the objects to be viewed get this small, of the order of a few tens of nanometers, the light that is used to view them become the limiting factor.

2 Sub-Diffraction-Limit Imaging

Imaging objects becomes more difficult as they get smaller because of the wavelength of light. Once two objects are separated by a distance of an order similar to that of the wavelength (λ) of the light used to view them, it is no longer possible to resolve these two objects apart, instead all that can be seen is a blur of the two objects together.

There have been several techniques developed for distinguishing objects apart on smaller and smaller scales. Many of these involve using different wavelengths of light. For example, instead of being limited by visible light, $\lambda \approx 5 \times 10^{-7}$ m, x-ray radiation ($\lambda \approx 10^{-10}$ m) or even electrons ($\lambda \approx 10^{-11}$ m) can be used to resolve smaller scales in x-ray and electron microscopy respectively. These, however, have the issue that, because the smaller wavelengths imply higher energies, there is the danger of destroying the sample.

The minimum distance that two objects can be resolved at is given by Abbe's criterion,

$$d = \frac{\lambda}{2NA} \quad (1)$$

$$= \frac{\lambda}{2n \sin \theta}, \quad (2)$$

where NA is the numerical aperture of the microscope, the range of angles that the microscope's lens will let light through properly. For $\lambda \approx 500$ nm (in the middle of the visible range), and $NA = 1.5$, the maximum resolving distance is $d = 160$ nm, this is the diffraction limit. This is an order of magnitude larger than the objects that need to be resolved. A few attempts to avoid this limit using exotic types of lenses have been developed [Fang et al., 2005], but these are currently far more expensive to use than traditional imaging equipment.

2.1 Image Manipulation

Instead of trying to avoid the diffraction limit using shorter wavelengths of light or other particles, other techniques employ different methods of actually capturing the image, or clever manipulation of the images that are produced, to get around the limitations of the diffraction problem.

For example Stochastic Optical Reconstruction Microscopy (STORM) [Rust et al., 2006] and PhotoActivation Localisation Microscopy (PALM) [Owen et al., 2010] use a technique where the objects to be imaged are molecules of a fluorescent dye. These are attached to the object of interest, a cell or sample of tissue for example. The type of dye molecule used allows the fluorescence to be switched on and off, allowing some markers to be imaged separately to others, effectively increasing the distance between points. Once an image is captured, the point spread function (PSF) of the point is used to locate the single marker, the "on" markers are changed and the image retaken. When many of these images are taken, they can be combined to provide accurate information on the original location of the markers and hence the shape and dimensions of the object.

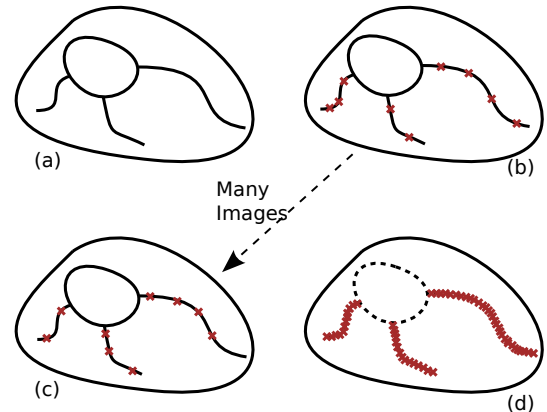


Figure 1: STORM imaging. (a) The actual structure to be imaged is too small for regular microscopy. In stages (b) through (c), many images are taken, each with a different subset of the fluorescent markers activated. When the images are combined, (d), the points add up and reveal the nature of the object.

3 Benchmarking

Throughout the project, a set of files will be used to test the algorithms that are developed; their correctness and effectiveness, speed and resource use. These files contain real data formatted in the same way as would be expected for data given to the plugin in general use. The files that will be used are detailed in Table 1.

Note that `palm-3-small.txt` is a subset of `palm-3.txt` which is used for simply checking correctness of algorithms. A summary of the columns that are included in the files, used and unused fields, is included in Appendix A.

File Name	Size	Points
palm-1.txt	12 MiB	65572
palm-2.txt	6.4 MiB	36672
palm-3.txt	5.8 MiB	33342
palm-3-small.txt	176 KiB	1000
uniform.txt	22 MiB	2000000

Table 1: These files containing sample data are used for benchmarking throughout the project.

Part II

Data Structures

The way in which data is represented in memory has a large effect on the speed, efficiency and effectiveness of any algorithms that are performed on that data. There are almost always a number of tradeoffs that must be considered when choosing or designing a data structure to hold data: speed of access vs. speed of search or traversal, storage space used vs. time to insert a datum, etc.

Some data structures may be naïvely chosen based on one of these, at the expense of the other. For example, consider storing the pixel information for a sparse image generated by a number of single pixel points—a linear array might be selected. This would give extremely good access and modification times, both $O(1)$, but insertion and deletion are very slow. There would also be a large amount of wasted space since every pixel that is black, i.e., does not have any points in, would need to have an array index with the same entry, 0.

1 Simple Grid Method

The simplest method for analysing the distribution of points is to use a regular grid of cells and place the points into the cells one at a time. Once all points have been added, the number of points per cell can be treated as a grey scale brightness value. This gives a simple pixel image, with brightness as a function of density of the points, in the `pnm` image format. A thresholding filter can then be applied to remove the points that are isolated and leave the denser areas corresponding to clusters.

Though the resolution of this method can be easily changed by altering the size of the cells and the grid, it performs badly when presented with data that is even slightly noisy. If the clusters themselves have a density that is not significantly above the background noise level, the thresholding step is prone to either exclude much of the real data, or to increase the size of the clusters by including too much noise. These two effects can be seen clearly in Figure 2, where `palm-1.txt` was used with a cell size of 200. The range of the data is from 0 to 41000 for both the x and the y axes, thus the images are 205 by 205 pixels. This data took 0.495s to generate.

There are steps that can be taken to improve the approach of this simple grid when handling outlying points caused by noise.

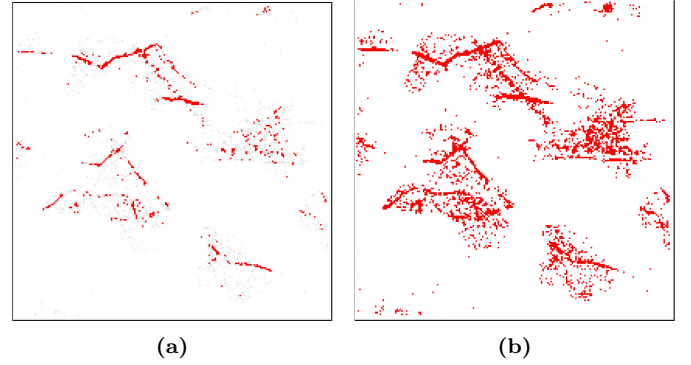


Figure 2: Setting a low threshold, (a), means that many of the points in the clusters are lost. Setting it higher, (b), includes too many of the points deemed to be noise. Pixels are cells that ended with points, red are points that would be kept by the threshold process, black would be removed.

1. First the algorithm is modified to include a thresholding step before writing the data to a file. This means that the pixels can be adjusted with greater accuracy and any arbitrary level can be chosen to threshold at.
2. Next, once an image has been generated, the number of points that contributed to each pixel is no longer of interest and so the image can be converted to a binary image. This is an image with just two possible values, the first represents white space, where there are no points, the second is black where there were points and so is of interest.
3. Once a binary image has been generated, erode and dilate filters can be applied to remove remaining outliers and to try to close the gaps in the structures that have been identified so that they are more solid.



Figure 3: Using a closing algorithm can help to emphasise the structure in the data and, at the same time, remove the isolated points representing noise.

These steps lead to significantly better isolation of the interesting parts of the image, as can be seen in Figure 3, however, much of the detail of the structure is lost in this process.

2 Quadrees

Since the simple grid method described in section 1 performs slowly and does not offer good cluster analysis, a different approach is needed. The chosen method is to use a quadtree data structure.

Quadrees are a type of recursive abstract data type in the form of a tree where every node has exactly zero or four children. A node with zero children is a leaf and contains some information, value or quantity. A node with four children is not a leaf and cannot hold information.

Quadrees are often used in image processing since the four children of the root node can naturally represent the four quadrants of the image; upper left, upper right, lower left and lower right. Since each of these children is also a quadtree, the image can be subdivided to any arbitrary depth. From this point, information about the image can be “seen” more easily by the computer and statistics calculated.

In order to identify a node uniquely in the tree, each node is given a code that is built up from its parent code plus some value that identifies it among its siblings. The root node is usually chosen to have an empty code so that the first four children are given the first level codes.

The choice of in what order to label the children is important if the order in which the nodes are placed is important. For spatial indexing, for example, each node represents a quadrant in two dimensional space, so being able to traverse the children in a sensible and predictable way is essential.

2.1 Morton Code (Z-Order)

Perhaps the most natural order to give to the values in a spatial quadtree is to number them from 1 to 4, left to right, top to bottom. This can be made more appropriate for a computer to use by numbering from 0 to 3. This is called Morton Order [Morton, 1966] or Z-order because of the resulting path that would be followed by traversing the nodes in order, Figure 4a. This has several useful features.

1. First, the numbers can be converted to base 2:
 - 0 becomes 00
 - 1 becomes 01
 - 2 becomes 10 and
 - 3 becomes 11.
2. This has advantages since binary is very efficient for computers to work with and allows certain tricks to be employed (see Morton order coordinates).
3. Also, this numbering system is easily extendible to any depth of tree that can be imagined.
 - (a) The root, as mentioned before, is given no value,
 - (b) each of the children are numbered 00 through 11.
 - (c) the children of these children are numbered 00 to 11 with the parent as a prefix. So the children of node 00 are 0000, 0001, 0010 and 0011. Likewise, the children of 11 are 1100, 1101, 1110 and 1111.

- (d) The children are always numbered in the same order. If starting at the top and going top to bottom and left to right, this is maintained for all children.

This method of numbering is simple and so acceptable for the standard uses of quadrees, but it was found to be difficult to work with in a spatial context when information about neighbouring cells is needed. The steps required to calculate the neighbours of any given cell are reasonably complex and so would add computational and time complexity to calculations performed on the tree.

2.2 Hilbert Order

One of the reasons the Z-order above becomes difficult to work with is that the resulting path from traversing the nodes in-order has to make large jumps and so cells which are numbered next to each other may, in fact, not be near each other in the image.

A number of routes exist that avoid this jumping around the image. These are based on space filling curves which have the property of being a simple recursive pattern that visits every point in a 2D space exactly once. These curves were first discovered in the early 1900's and described mathematically by D. Hilbert [Hilbert, 1970]. One of the curves that Hilbert found, the Hilbert Curve, is particularly useful since it can be represented in the simplest level in a two by two square which is then recursively repeated for each quadrant of that first square—exactly as the quadtree does.

The path that the traversal of points follows becomes fairly complicated, Figure 4b. This means, again, that the calculation of neighbours becomes difficult.

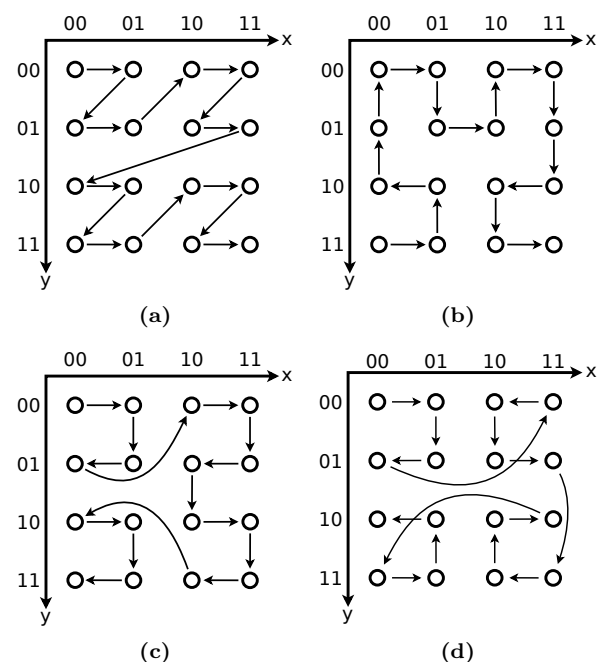


Figure 4

2.3 Gray Codes

The Gray Code [GRAY, 1953], developed by Frank Gray in 1953, was originally designed to reduce the error rate produced by mechanical electronics. The code is a variation on binary where each step when counting up changes only a single bit at a time. This meant that electromechanical apparatus was less likely to make a mistake or generate errors since the actions required to count from one to two required only a single bit change, rather than two, as would be required for binary counting. When using just two bits, i.e., counting from zero to three, the steps are very similar to binary, (00, 01, 11, 10).

The path that this follows is shown in Figure 4c. This does not seem to provide any benefits since there is now more jumping around the image space than with Z-order and the neighbours are just as difficult to calculate as for Hilbert Order. However, by using a different arrangement of the sub-trees, as the Hilbert curve does, the leaf nodes group themselves in a very ordered fashion. When arranged as in Figure 4d and 5, each cell is arranged such that

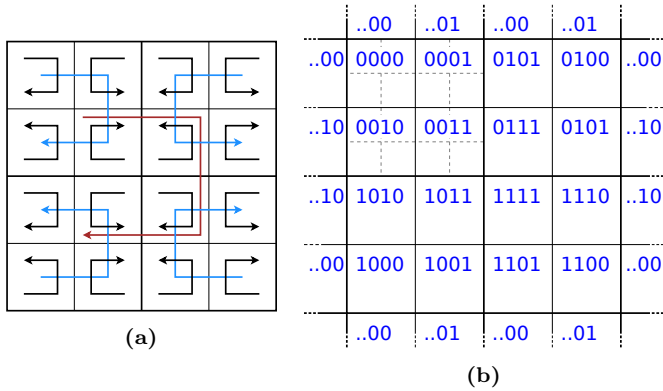


Figure 5

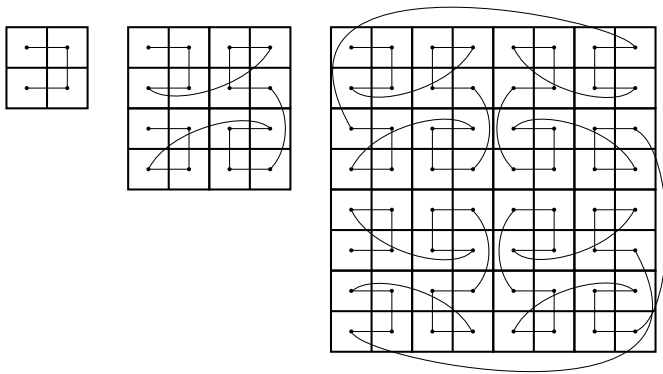


Figure 6: *modgray-Steps*

Since the quadtree is a recursive data structure, it is necessary to be able to maintain the correct orientation of child trees with respect to their parents at the construction stage. It turns out that this is easy to achieve and thus adapting it for each of the arrangements discussed above is simply a matter of adjusting the next part of the code that is added for each of the four children when creating them. Pseudo code to achieve this for the Morton order and the modified Gray code order is shown in Listing 1.

```
// Constructor
Quadtree(max_x, max_y, code)

// Child creation, Z-Order
t_l = new Quadtree(100, 100, this.code + "00");
t_r = new Quadtree(100, 100, this.code + "01");
b_l = new Quadtree(100, 100, this.code + "11");
b_r = new Quadtree(100, 100, this.code + "10");

// Child creation, Gray Code
t_l = new Quadtree(100, 100, this.code + "00");
t_r = new Quadtree(100, 100, this.code + "01");
b_l = new Quadtree(100, 100, this.code + "10");
b_r = new Quadtree(100, 100, this.code + "11");

// Child creation, Modified Gray Code
if (pos == "tl") {
    new_code[0] = code + "00";
    new_code[1] = code + "01";
    new_code[2] = code + "10";
    new_code[3] = code + "11";
} else if (pos == "tr") {
    new_code[0] = code + "01";
    new_code[1] = code + "00";
    new_code[2] = code + "11";
    new_code[3] = code + "10";
} else if (pos == "bl") {
    new_code[0] = code + "10";
    new_code[1] = code + "11";
    new_code[2] = code + "00";
    new_code[3] = code + "01";
} else if (pos == "br") {
    new_code[0] = code + "11";
    new_code[1] = code + "10";
    new_code[2] = code + "01";
    new_code[3] = code + "00";
}
t_l = new Quadtree(100, 100, this.code + new_code[0]);
t_r = new Quadtree(100, 100, this.code + new_code[1]);
b_l = new Quadtree(100, 100, this.code + new_code[2]);
b_r = new Quadtree(100, 100, this.code + new_code[3]);
```

Listing 1: Code to generate children of the current quadtree while maintaining the correct ordering.

2.4 Quadtree Definitions

It is useful to define a few terms that shall be used in the context of quadtrees. Many of these are identical to the definitions more commonly applied to binary trees.

Root The node at the topmost position in the tree.

Child One of the four nodes that are beneath a given node for which there is a direct path of length 1 between this node and it.

Height The length of the longest path from the root node to one of the leaf nodes.

Depth The length of the path from a given node up to the root.

Completeness A quadtree is ‘complete’ when each of the root node’s four children have the same height. In this case, the number of leaves in the tree is a maximum.

3 Cluster Analysis

Cluster analysis is the grouping of a set of objects or items in a spatially or informationally logical way such that the items that are placed in the same group are more similar to each other than they are to the objects in the other groups in the set. These groups are called clusters. When dealing with images, the clustering that is of interest is based on spatial location, i.e., clusters should be composed of objects that are close together in the image and clusters should be separated by regions of emptiness or background level noise.

One of the primary reasons for choosing the quadtree method over the simple grid methods was that the simple act of placing the objects, in this case coordinates of data points, into the quadtree starts the process of analysing the data. Since the points end up in a tree structure with the number of points closely separated being on the lowest levels of the tree, the data is already clustered in a way.

There are a number of alternative methods of identifying clusters in images.

3.1 Rolling Ball Analysis

The accessible surface area algorithm, also known as the “Rolling Ball Method”, is a technique used in image processing for describing the outer limit of a cluster of points. It is derived from biological molecules analysis where it describes surface area of a molecule that is accessible to a solvent.

The rolling ball method can be used to analyse a cluster of points by imagining a ball that sits against one of the outermost points. From here it is “rolled” around the cluster such that it is always touching at least one point. Once the ball has reached the point it started at, the line that the ball traced is reduced in size by the radius of the ball. This line then represents the outer limit of the cluster.

The size of the ball must be chosen depending on the average separation of the points within the cluster.

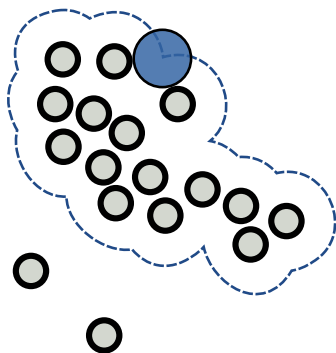


Figure 7: *rolling-Ball*

4 Quadtree Traversal

When discovering clusters via this propagation technique, care must be taken to avoid a run-away situation where every node in the tree gets included. This would happen when looking at

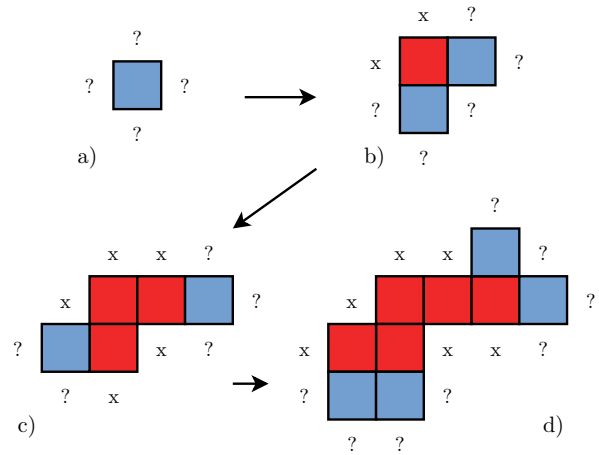


Figure 8: *Propagation*

the neighbours of a node and blindly including them. Since every internal node has exactly four neighbours, the propagation would terminate only when reaching the edge nodes.

Instead, the depth of the node must be considered. Again, the simplest method is not sufficient. If the propagation is limited to a given node depth, even if this is not the same as the deepest node, the size of any clusters that are identified will be limited, as shown in Figure 9. Since the depth to consider is not able to change, when the neighbours of the blue cell are checked, no correct neighbours are found and so the process terminates. When able to view the larger structure of the cells, however, it is clear that the structure continues beyond the gap.

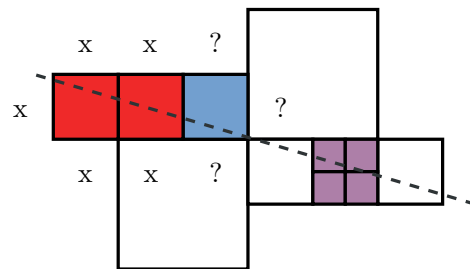


Figure 9: *propagation-Halting*

To avoid this, a certain amount of leniency must be given when deciding what constitutes a neighbour. Given an appropriate value, this would allow both of the larger white cells in Figure 9 to be included.

The *depth range* shall define the levels that are to be considered when choosing neighbours with respect to a target depth. Since clusters are being considered areas of increased density of points, all cells with a depth greater than the target depth shall be allowed, so the purple cells in Figure 9 would be included when the target depth is the same as the depth of the included red cells. A depth range of zero is equivalent to the situation above where only cells of a given depth are considered. A depth range of 1 would mean that the white square in Figure 10 b) would be included but not in c), whereas a depth range of three would include both.

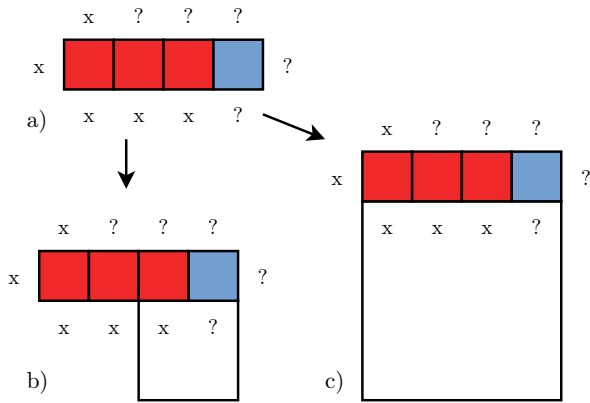


Figure 10: *propogation-Levels*

Part III

ImageJ Plugin

1 ImageJ

Imagej is an public domain, Java based image manipulation program written and maintained by developers at the National Institute of Health. It is widly used in medical and biological research and has an open API to allow extension via macros, plugins and scripts.

Since they offer significantly betting integration, meaning speed and efficiency improvements, a plugin is chosen to integrate this project into ImageJ over macros, which suffer per-ormace loss when more than a few steps are involved, and scripts which do not offer such tight integration with the rest of the program.

The plugin shall allow a user to load a data set, as gathered from STORM, PALM or similar imaging techniques discussed in Section 2, choose the format of the data (the columns that are of interest etc.) analyse the data for clusters and receive detailed information regarding the clusters that were found.

2 ImageJ Plugin

The first version of the plugin simply allowed the user to visualise the data, once it had been processed and entered into a quadtree. Though this provided little benefit to the researcher producing data, it can be useful to simply get an insight into the process that a program is using to analyse one's data so that the results can be better interpreted. For this reason, this version served as a foundation for later versions of the plugin so that, when loading data, a user gets the opportunity to view the data before proceding with the analysis.

The analytical steps that are undertaken are descibed in more detail in later sections.

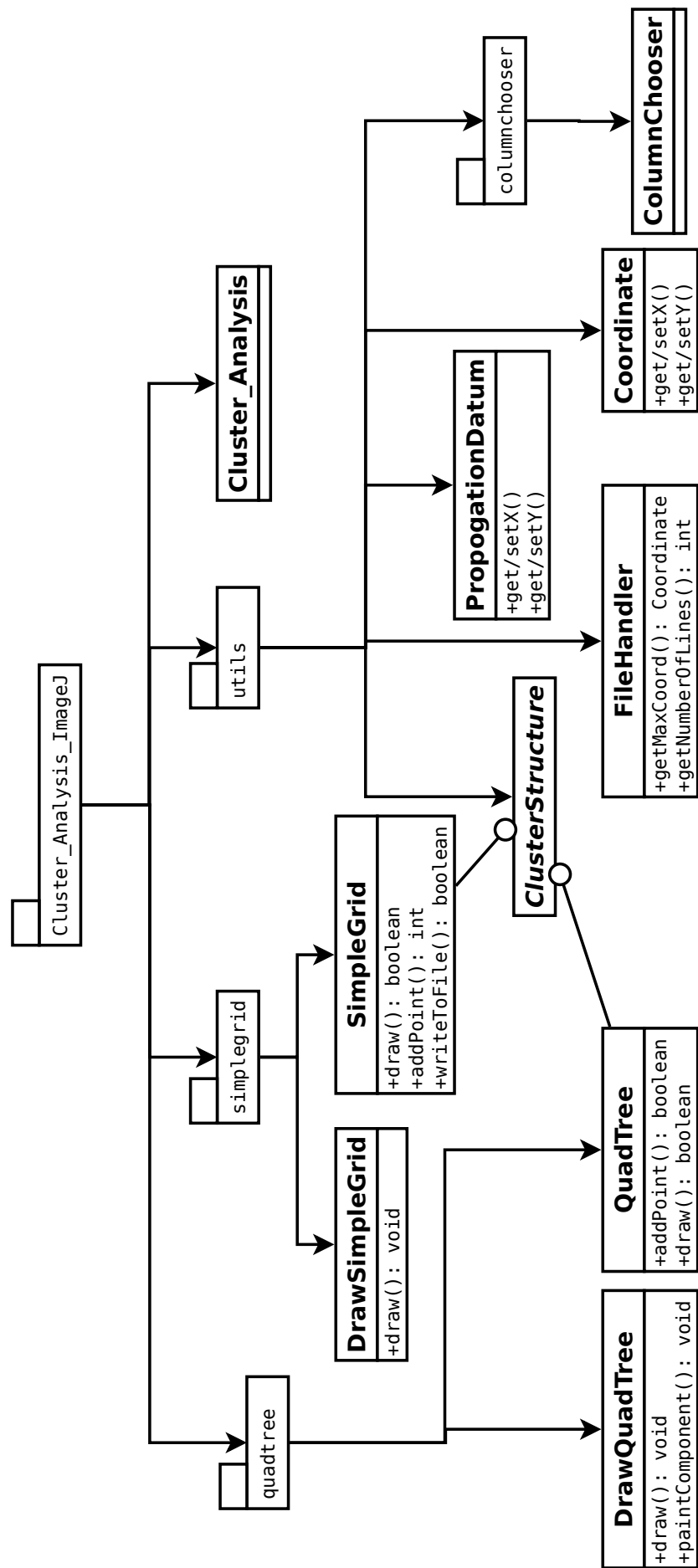


Figure 11: Name

A Data File Structure

The data files that are produced from the initial analysis of the images have a standard format.

1. Tab separated fields.
2. Single header line with names of fields.
3. One or more item of data, separated by newlines.

The columns that represent fields in the file are as follows.

Header	Meaning	Used?
Channel Name	Wavelength channel that was used to capture data. First value, I , is the incident wavelength of the light used to excite the dye and the second, E , is the wavelength emitted that was imaged.	no
X	x-coordinate of the point	no
Y	y-coordinate of the point	no
Xc	centered, normalised x-coordinate of point	yes
Yc	centered, normalised y-coordinate of point	yes
Height	the height of the fitted gaussian peak used to extract the point from the original image	not yet
Area	area of the point	not yet
Width	full width half maximum of the point	not yet
Phi	?	no
Ax	?	no
BG	?	no
I	?	no
Frame	?	no
Length	?	no
Valid	?	no
Z	?	no
Zc	?	no
Photons	?	no
Lateral Localisation Accuracy	?	no
Xw	?	no
Yw	?	no
Xwc	?	no
Ywc	?	no

References

- [Asano et al., 1997] Asano, T., Ranjan, D., Roos, T., Welzl, E., and Widmayer, P. (1997). Space-filling curves and their use in the design of geometric data structures. *Theoretical Computer Science*, 181(1):3–15.
- [Fang et al., 2005] Fang, N., Lee, H., Sun, C., and Zhang, X. (2005). Sub-diffraction-limited optical imaging with a silver superlens. *Science*, 308(5721):534–537.
- [GRAY, 1953] GRAY, F. (1953). Pulse code communication. US Patent 2,632,058.
- [Hess et al., 2006] Hess, S. T., Girirajan, T. P., and Mason, M. D. (2006). Ultra-high resolution imaging by fluorescence photoactivation localization microscopy. *Biophysical journal*, 91(11):4258–4272.
- [Hilbert, 1970] Hilbert, D. (1970). Über die stetige abbildung einer linie auf ein flächenstück. In *Gesammelte Abhandlungen*, pages 1–2. Springer.
- [Hjaltason and Samet, 2002] Hjaltason, G. R. and Samet, H. (2002). Speeding up construction of pmr quadtree-based spatial indexes. *The VLDB Journal—The International Journal on Very Large Data Bases*, 11(2):109–137.
- [Mokbel et al., 2002] Mokbel, M. F., Aref, W. G., and Kamel, I. (2002). Performance of multi-dimensional space-filling curves. In *Proceedings of the 10th ACM international symposium on Advances in geographic information systems*, pages 149–154. ACM.
- [Morton, 1966] Morton, G. (1966). A computer oriented geodetic data base and a new technique in file sequencing. *IBM, Ottawa, Canada*.
- [Owen et al., 2010] Owen, D. M., Rentero, C., Rossy, J., Magenau, A., Williamson, D., Rodriguez, M., and Gaus, K. (2010). PALM imaging and cluster analysis of protein heterogeneity at the cell surface. *Journal of biophotonics*, 3(7):446–454.
- [Rasband, 1997] Rasband, W. (1997). ImageJ, US National Institutes of Health. *Bethesda, Maryland, USA*, 2012.
- [Rust et al., 2006] Rust, M. J., Bates, M., and Zhuang, X. (2006). Sub-diffraction-limit imaging by stochastic optical reconstruction microscopy (STORM). *Nature methods*, 3(10):793–796.
- [Samet, 1990] Samet, H. (1990). Applications of spatial data structures. *Computer Graphics, Image Processing, and GIS*.
- [van Oosterom, 1999] van Oosterom, P. (1999). Spatial access methods. *Geographical information systems*, 1:385–400.
- [Williamson et al., 2011] Williamson, D. J., Owen, D. M., Rossy, J., Magenau, A., Wehrmann, M., Gooding, J. J., and Gaus, K. (2011). Pre-existing clusters of the adaptor lat do not participate in early t cell signaling events. *Nature immunology*, 12(7):655–662.